Circ J 2017; 81: 846–854
doi:10.1253/circj.CJ-16-1162

ORIGINAL ARTICLE
Pediatric Cardiology and Adult Congenital Heart Disease

Mechanisms of Left Ventricular Dysfunction Assessed by Layer-Specific Strain Analysis in Patients With Repaired Tetralogy of Fallot

Mariko Yamada, MD; Ken Takahashi, PhD; Maki Kobayashi, PhD; Kana Yazaki, MD; Hirobumi Takayasu, PhD; Katsumi Akimoto, MD; Masahiko Kishiro, MD; Akio Inage, MD; Tadahiro Yoshikawa, MD; In-Sam Park, PhD; Keisuke Nakanishi, PhD; Shiori Kawasaki, PhD; Toshiaki Shimizu, PhD

Background: Left ventricular (LV) dysfunction in patients with repaired tetralogy of Fallot (rTOF) is an important risk factor for adverse outcomes. The aim of this study was to assess the details and time course of such LV dysfunction using layer-specific strain analysis by echocardiography.

Methods and Results: The 66 patients with rTOF (mean age, 16.3±9.3 years) were divided into 3 groups (T1: 4–10 years, T2: 11–20 years, T3: 21–43 years), and 113 controls of similar age (mean age, 17.2±9.3 years) were divided into 3 corresponding groups (C1, C2, and C3). Layer-specific longitudinal strain (LS) and circumferential strain (CS) of 3 myocardial layers (endocardial, midmyocardial, and epicardial) were determined by echocardiography. Basal and papillary endocardial CS values were decreased in T1 compared with C1. With the exception of papillary epicardial CS, basal/papillary CS and LS of all 3 layers decreased in T2 compared with C2. Excepting papillary epicardial CS, all other values were decreased in T3 compared with C3.

Conclusions: Potential myocardial damage was found in the endocardium at the basal and papillary levels of the LV in young patients with rTOF, extending from the endocardium to the epicardium and from the base to the apex. This is the possible time course of LV dysfunction in patients with rTOF.

Key Words: Echocardiography; Layer-specific strain; Myocardial deformation; Tetralogy of Fallot

Tetralogy of Fallot (TOF) is the most prevalent form of cyanotic congenital heart disease.[1] Significant advances in the early management of TOF have dramatically improved the survival of TOF patients,[2] with current 30-year survival rates reaching 89%.[3] However, late ventricular dysfunction related to residual hemodynamic and electrophysiological abnormalities remains a problem, contributing to increasing morbidity and mortality rates beginning in the third decade of life.[2,4–6] Previous investigators assessing ventricular function in patients with repaired TOF (rTOF) have primarily focused on right ventricular (RV) mechanics and their interaction with pulmonary regurgitation (PR).[7–9] Moreover, the importance of left ventricular (LV) dysfunction as a risk factor for long-term adverse outcomes is increasingly acknowledged.[8,10–12] Davlouros et al found a significant correlation between RV ejection fraction (EF) and LVEF, and highlighted the importance of LV-RV interaction in patients who have undergone TOF repair.[8] Geva et al showed that lower LVEF and older age at repair were the strongest independent factors associated with impaired clinical status in long-term survivors of rTOF.[13] Recently, Diller et al showed that LV longitudinal dysfunction, such as impairment in longitudinal global strain and decreased mitral annular plane systolic excursion, were associated with an increased risk of sudden cardiac death and/or life threatening ventricular arrhythmias in patients with rTOF.[12] Therefore, the assessment of LV function in patients with TOF is crucial because it is the strongest determinant of a poor clinical outcome in these patients. Despite the importance of LV dysfunction, the mechanisms and time course of the development of LV dysfunction remain poorly understood.[14] Its mechanisms and time course in patients with rTOF are important because it has the potential to become

Received November 15, 2016; revised manuscript received February 6, 2017; accepted February 9, 2017; released online March 3, 2017 Time for primary review: 34 days

Department of Pediatrics and Adolescent Medicine, Juntendo University Graduate School of Medicine, Tokyo (M.Y., K.T., M. Kobayashi, K.Y., H.T., K.A., M. Kishiro, T.S.); Department of Pediatric Cardiology, Sakakibara Heart Institute, Tokyo (A.I., T.Y.); Department of Pediatric Cardiology, Tokyo Women's Medical University, Tokyo (I.-S.P.); and Department of Cardiovascular Surgery, Juntendo University Faculty of Medicine, Tokyo (K.N., S.K.), Japan

Mailing address: Ken Takahashi, PhD, Department of Pediatrics and Adolescent Medicine, Juntendo University Graduate School of Medicine, 2-1-1 Hongo, Bunkyo-ku, Tokyo 113-8421, Japan. E-mail: kentaka@juntendo.ac.jp

ISSN-1346-9843

a novel indicator capable of detecting cardiac dysfunction with a high sensitivity.

A recent development is layer-specific strain analysis, which allows separate quantification of deformation for the endocardial, midmyocardial, and epicardial layers of the myocardium.[15] The usefulness of this new sensitive indicator for detecting cardiac dysfunction in various cardiac diseases has been reported.[15–17]

To the best of our knowledge, no previous study has analyzed layer-specific deformation of the LV in patients with rTOF, so our aim was to assess the details and time course of LV dysfunction in patients with rTOF using layer-specific strain analysis.

Methods

Study Population

We prospectively recruited 66 patients (age, 4–43 years) who had rTOF and were scheduled for elective outpatient echocardiography. Patients with residual intracardiac shunts, known ventricular arrhythmias, and implanted pacemakers were excluded. Clinical data, including demographics, age at surgery, type of RV outflow reconstruction, and whether ventriculotomy was performed, were obtained from the medical records. LV strain analysis was performed in all patients. A group of healthy subjects of a similar age was recruited as controls for LV myocardial mechanical analysis. Controls were either healthy volunteers or children undergoing echocardiography for the evaluation of innocent murmurs who had no history of cardiovascular disease, showed normal sinus rhythm on ECG, and normal findings on echocardiography. All participants or their guardians provided informed consent, as established by the Research Ethics Board at Juntendo University. To identify the characteristics of myocardial deformation in patients with rTOF more clearly, patients were divided into 3 groups according to age: T1, <11 years old; T2, 11–20 years old; T3, 21–43 years old. Controls were also divided into 3

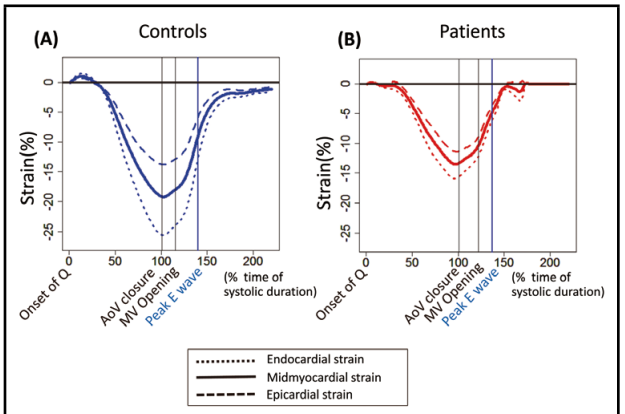

Figure 1. Examples of typical LV layer-specific strain curves for papillary endocardial, midmyocardial, and epicardial circumferential strain in normal controls (**A**) and patients with repaired tetralogy of Fallot (**B**). Negative end-systolic strain represents myocardial shortening during systole. Progressive decrease in systolic strain from the endocardial to epicardial layer is seen in both the patients and controls; the maximal difference is seen at the time of peak strain. The basic form of the strain curves did not differ significantly between the controls and patients, though the peak strain had a significant difference, as shown. The timing of peak strain in the controls and in patients is near closure of the aortic valve (AoV), decreasing rapidly during early diastole in each layer. LV, left ventricle; MV, mitral valve.

Table 1. Baseline Characteristics of Study Group of Patients With Repaired Tetralogy of Fallot (T1–T3) and Healthy Controls (C1–C3)

	T1	T2	T3	C1	C2	C3
n (male)	20 (11)	25 (16)	21 (11)	37 (21)	37 (19)	39 (21)
Age (years)	7.01±0.82††,‡‡	14.12±0.73	27.8±0.8††	8.03±0.60††,‡‡	14.42±0.60	28.4±0.5††
HR	81.1±15.3††,‡‡	67.6±10.2	65.9±8.9	75.1±11.3††,‡‡	65.0±9.3	62.5±7.6
QRS duration	124.1±23.1**,‡	131.5±26.5**	141.5±34.9**	91.1±8.2	94.3±13.3	96.5±10.1
RVEDA/BSA	17.0±4.4**	15.7±5.1**	14.5±4.7**	9.42±2.88	10.7±3.4	8.28±2.26
RVESA/BSA	8.65±3.55**	7.94±3.48*	8.10±3.57**	4.30±1.73	5.50±2.09	3.87±1.52
RVFAC	50.7±11.8	50.0±9.2	45.5±8.5*	54.9±7.4	49.4±8.6	53.9±8.7
RVFAC <35% (n)	2	0	3*	0	2	1
LVEDV/BSA	49.9±8.9	52.1±15.5	43.8±9.6	45.4±10.8	53.1±14.2	49.6±8.9
LVESV/BSA	18.1±4.1	18.1±6.3	16.9±4.6	15.2±4.6	18.5±5.9	18.3±4.6
LVEF	63.7±4.8	65.5±3.9	61.6±5.2	66.8±3.7	65.2±5.0	63.7±5.5
LVEF <55% (n)	1	0	1	0	1	1
Mitral E velocity	1.10±0.22‡	1.14±0.21	0.92±0.28†	1.05±0.15‡‡	1.02±0.17	0.87±0.13†
Mitral E/A	2.62±1.07	2.87±0.72*	2.22±0.87†	2.42±0.47‡‡	2.25±0.53	1.78±0.38†
Septal e'	10.0±2.8**	10.8±3.3**	8.8±2.9**	14.5±2.2	15.0±2.9	13.5±2.0
LV FW e'	14.0±4.1**	14.4±5.0**	13.1±3.7*	19.0±2.9	19.3±2.9	16.9±2.7†
Septal E/e'	11.8±3.6**	11.5±4.1**	11.5±5.0**	7.42±1.65	7.0±1.6	6.55±1.44
LV FW E/e'	8.76±3.64**	8.44±2.15**	7.35±2.24**	5.63±1.17	5.37±1.09	5.23±0.96

*Patients after TOF repair vs. controls with corresponding age groups, P<0.05. **Patients after TOF repair vs. controls with corresponding age groups, P<0.01. †Significant difference between adjacent age groups, P<0.05. ††Significant difference between adjacent age groups, P<0.01. ‡Significant difference between T1 and T3 or C1 and C3, P<0.05. ‡‡Significant difference between T1 and T3 or C1 and C3, P<0.01. T1: 4–10 years old, T2: 11–20 years old, T3: 21–43 years old; C1–3, control groups of similar ages. BSA, body surface area; HR, heart rate; FW, free wall; LVEDV, left ventricular end-diastolic volume; LVEF, left ventricular ejection fraction; LVESV, left ventricular end-systolic volume; RVEDA, right ventricular end-diastolic area/body surface area; RVESA, right ventricular end-systolic area; RVFAC, right ventricular fractional area change.

Table 2. Characteristics of Study Patients With Repaired Tetralogy of Fallot

Characteristics	T1	T2	T3
Mean age at repair (years)	1.52±0.84††	1.47±0.87	4.0±1.5**
Duration from the repair (years)	5.48±1.45**	12.4±2.7	23.6±5.9**
Severe PR (n)	6	3	2
Moderate PR (n)	9	13	10
Mild PR (n)	5	8	9
Trivial PR (n)	0	1	0
TAP (n)	11	16	13
Non-TAP (n)	8	5	5
Rastelli (n)	1	4	2
Previous shunt surgery (n)	4	4	3
Ventriculotomy (n)	2	2	0
ARB (n)	2	6	1
ACEI (n)	2	7	0
β-blocker (n)	0	0	1
α-β-blocker (n)	1	0	4
PDE5 inhibitor (n)	0	0	1
Diuretics (n)	0	0	2
Residual VSD (n)	0	0	0
Secondary PVR (n)	0	0	1
PG at RVOT	13.9±4.1*,†	26.0±13.8	24.9±12.0

Data are expressed as mean ± SD. *Significant difference between adjacent age groups, P<0.05. **Significant difference between adjacent age groups, P<0.01. †Significant difference between T1 and T3 or C1 and C3, P<0.05. ††Significant difference between T1 and T3 or C1 and C3, P<0.01. T1: 4–10 years old, T2: 11–20 years old, T3: 21–43 years old. ACEI, angiotensin-converting enzyme inhibitor; ARB, angiotensin II receptor blocker; PDE, phosphodiesterase; PR, pulmonary regurgitation; PVR, pulmonary valve replacement; RVOT at PG, pressure gradient at right ventricular outflow tract; TAP, transannular patch; VSD, ventricular septal defect.

groups (C1, C2, and C3) according to the same age groupings.

Echocardiography

Echocardiography was performed using a Vivid E7 or Vivid E9 ultrasound system (GE Healthcare, Milwaukee, WI, USA) with an M5 or M4S probe for Vivid E7, and an M5S or 6S probe for Vivid E9, as appropriate for the patient's size. Images were optimized for gain, compression, depth, and sector width and acquired at frame rates of 70–125 frames/s. Apical 4- and 2-chamber views and parasternal short-axis views at the basal, papillary, and apical ventricular levels were acquired. In each plane, images from 3 consecutive cardiac cycles were acquired during a breath hold at end-expiration, if possible. For younger children, we selected 3 cardiac cycles at end-expiration on the respiratory trace.

The mitral inflow E-wave, A-wave, and E/A ratio were measured. The degree of PR was assessed by measuring the jet size using color Doppler, jet density, and deceleration rate with continuous wave and pulmonary systolic flow compared with systemic flow using pulse-wave Doppler.[18] The pressure gradient at the RV outflow tract (RVOT) was estimated by the peak continuous-wave Doppler velocity of the RVOT. RV end-diastolic area (RVEDA) and RV end-systolic area (RVESA) were measured in the apical 4-chamber view by tracing the endocardial border of the RV and the tricuspid annular plane.[19] The RV fractional area change (RVFAC) was calculated as (RVEDA−RVESA)/RVEDA. LV end-diastolic volume (LVEDV) and LV end-systolic volume (LVESV) were calculated from the apical 4-chamber and 2-chamber views using the modified Simpson rule. LVEF was calculated as (LVEDV−LVESV)/LVEDV. LV diastolic function was quantified using the ratio between the E-wave velocity of the pulsed wave Doppler mitral flow and the early diastolic velocity of the septum and LV free wall at the mitral annulus level (e' wave) on tissue Doppler imaging.

LV Deformation Analysis

Analysis was performed offline with the aid of a commercially available software package (EchoPAC 113 1.0; GE Vingmed Ultrasound AS, Horton, Norway). Strain analysis was performed by 2 observers (M.Y. and K.Y.) blinded to the clinical data. Strain was measured using 2D speckle-tracking echocardiography. The LV endocardium was manually traced, and the region of interest was manually adjusted to the LV wall thickness. The software tracks myocardial motion through the cardiac cycle, calculating strain from echogenic speckles in the B-mode image. From the basal, papillary, and apical short-axis data and apical 4-chamber view, 1 cardiac cycle was selected for subsequent analysis. All data were measured at least 3 times, and the averages are reported. The system used for this study allows calculation of mean strain values for total wall thickness and for 3 separate myocardial layers (endocardial, papillary, and epicardial), as described previously (**Figure 1**).[20] LV apical rotation, basal rotation, and torsion were analyzed as described previously.[21] All data were measured at least 3 times, and the averages are reported.

Statistical Analysis

Data are expressed as a mean (standard deviation [SD]). LV layer-specific strain and torsion data were compared

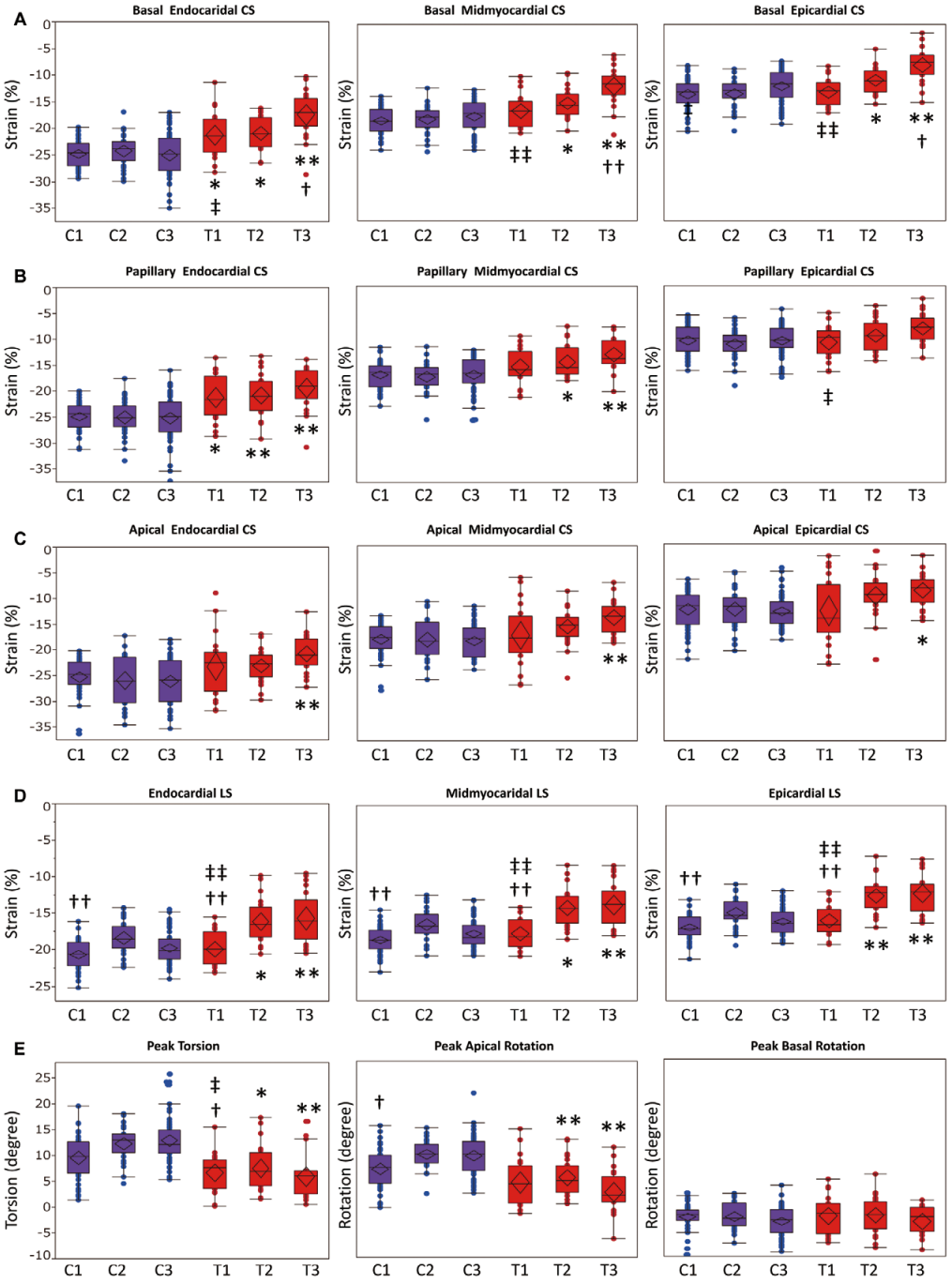

Figure 2. Comparison of the LV layer-specific strain analysis of (**A**) basal circumferential strain (CS), (**B**) papillary CS, (**C**) apical CS, (**D**) longitudinal strain (LS), and (**E**) torsion, apical rotation, and basal rotation. Blue, normal controls (C); red, patients (T) with repaired tetralogy of Fallot (rTOF). *Patients with rTOF vs. controls with corresponding age groups, P<0.05. **Patients with rTOF vs. controls with corresponding age groups, P<0.01. †Significant difference between adjacent age groups, P<0.05. ††Significant difference between adjacent age groups, P<0.01. ‡Significant difference between T1 and T3 or C1 and C3, P<0.05. ‡‡Significant difference between T1 and T3 or C1 and C3, P<0.01. T1: 4–10 years old, T2: 11–20 years old, T3: 21–43 years old; C1–3, control groups of similar age.

between patients with rTOF and controls using 1-factor analysis of variance with posthoc comparison. The correlation between RVFAC/RVEDA/RVESA and each value was evaluated by linear regression analysis.

Intraobserver and interobserver agreements for the LV layer-specific strain were calculated using the Bland-Altman approach, including the calculation of mean bias (average difference between measurements), and the lower and

Table 3. Correlation Between RV Function and LV Deformation Parameters

	RVEDA index		RVESA index		RVFAC	
	r	P value	r	P value	r	P value
Api						
Endo	0.25	<0.001	0.28	<0.001	−0.28	0.002
Mid	0.31	<0.001	0.35	<0.001	−0.28	<0.001
Epi	0.32	<0.001	0.35	<0.001	−0.24	0.001
Pap						
Endo	0.34	<0.001	0.33	<0.001	−0.22	0.003
Mid	0.27	<0.001	0.28	<0.001	−0.22	0.003
Epi	0.13	0.091	0.17	0.021	−0.17	0.020
Bas						
Endo	0.39	<0.001	0.39	<0.001	−0.027	<0.001
Mid	0.30	<0.001	0.32	<0.001	−0.23	0.002
Epi	0.16	0.034	0.19	0.010	−0.15	0.038
Long						
Endo	0.28	<0.001	0.34	<0.001	−0.31	<0.001
Mid	0.30	<0.001	0.35	<0.001	−0.32	<0.001
Epi	0.31	<0.001	0.36	<0.001	−0.31	<0.001
Rotation						
Torsion	−0.43	<0.001	−0.39	<0.001	0.20	0.007
Api rot	−0.48	<0.001	−0.44	<0.001	0.23	0.002
Bas rot	−0.04	0.592	−0.06	0.453	0.09	0.232

Correlation coefficients refer to non-parametric Spearman rank coefficients (r). Statistically significant P<0.05. Api, apical; Bas, basal; Long, longitudinal; Pap, papillary; Endo, endocardial; Epi, epicardial; Mid, midmyocardial; Rot, rotation. Other abbreviations as in Table 1.

upper limits of agreement (95% limits of agreement of mean bias) in 5 randomly selected patients and 5 controls at greater than 2 months apart. In addition, the coefficient of variation was determined (i.e., the SD of the difference of paired samples divided by the average of the paired samples). Statistical analyses were performed using JMP, version 9.0.2 software (SAS Institute Inc., Cary, NC, USA). P<0.05 was considered statistically significant. All data were measured at least 3 times, and the averages are reported.

Results

Feasibility

We excluded 6 patients and 5 controls because of inadequate data in the parasternal short-axis views and apical 2-chamber and 4-chamber views. In total, 179 subjects, comprising 66 patients with rTOF (mean age, 16.3±9.3 years) and 113 healthy controls (mean age, 17.2±9.3 years) were included from February 2010 to July 2016. **Tables 1** and **2** present the characteristics of the study participants. All patients were in sinus rhythm. All except 1 patient were classified as having New York Heart Association (NYHA) functional class 1 without any clinical symptoms; the 1 patient was classified as NYHA functional class 2. As shown in **Table 2**, 24 (36.4%) patients were on medication. Surgical repair techniques are also listed in **Table 2**; information about the surgical procedure was unavailable for 1 patient. The mean RV outflow pressure gradient was significantly lower in the T1 group than in the T2 and T3 groups. The RVEDA/body surface area (BSA) and RVESA/BSA were significantly larger in all TOF groups than in the control groups of corresponding age. RVFAC was significantly decreased in the T3 group compared with the C3 group, although only 5 of 66 patients showed an RVFAC below the normal range (23.9–34.4%), when the normal RVFAC range was defined as >35%.[19] There were no significant differences in the LVEF, LVEDV/BSA, and LVESV/BSA between patients and controls (**Table 1**). The LVEF in 2 (3.0%) patients was below the normal range (48.8% and 49.5%, respectively), when the normal LVEF range was defined as >55%.[19] E/e' at the septal and LV free walls were significantly higher in the TOF groups of all ages than in the control groups (P<0.001). E/A was significantly higher in the T2 group than in the C2 group.

LV Circumferential Strain (CS) Patterns

Basal Peak endocardial basal CS was decreased in the rTOF groups of all ages compared with the control groups (**Figure 2**, **Table S1**). Peak midmyocardial and epicardial basal CS values were decreased in the T2 and T3 groups compared with the C2 and C3 groups.

Papillary Peak endocardial papillary CS was decreased in the rTOF groups of all ages compared with the control groups (**Figure 2**, **Table S1**). Peak midmyocardial papillary CS was decreased in the T2 and T3 groups compared with the C2 and C3 groups. Peak epicardial papillary CS was not significantly different between the groups.

Apical Peak apical CS in all 3 layers was decreased only in the T3 group compared with the C3 group (**Figure 2**, **Table S1**). There were no significant differences in the apical CS in the T1 and T2 groups compared with the C1 and C2 groups.

Longitudinal Strain (LS) Pattern

Peak LS in all 3 layers was decreased in the T2 and T3 groups compared with the C2 and C3 groups (**Figure 2**, **Table S1**).

Table 4. Intraobserver and Interobserver Variabilities of Layer-Specific Strain

Variable	Bias	LLA	ULA	CV
Intraobserver				
Endocardial basal CS	0.733	−0.138	1.605	1.83
Midmyocardial basal CS	0.344	−0.535	1.223	2.52
Epicardial basal CS	0.046	−1.162	1.255	4.90
Endocardial papillary CS	0.650	−0.733	2.033	2.90
Midmyocardial papillary CS	0.355	−0.935	1.644	3.75
Epicardial papillary CS	0.169	−1.186	1.523	5.78
Endocardial apical CS	0.083	−5.148	5.314	10.2
Midmyocardial apical CS	0.357	−2.986	3.700	8.88
Epicardial apical CS	0.603	−1.827	3.033	8.96
Endocardial LS	0.297	−0.459	1.052	2.07
Midmyocardial LS	0.307	−0.330	0.944	1.93
Epicardial LS	0.339	−0.240	0.917	1.93
Torsion	0.357	−2.986	3.700	8.88
Interobserver				
Endocardial basal CS	0.120	−0.906	1.146	2.12
Midmyocardial basal CS	0.004	−0.945	0.952	2.69
Epicardial basal CS	−0.130	−0.812	0.551	2.75
Endocardial papillary CS	−0.007	−1.963	1.950	4.05
Midmyocardial papillary CS	−0.107	−1.111	0.896	2.88
Epicardial papillary CS	−0.148	−0.980	0.684	3.50
Endocardial apical CS	−0.100	−3.938	3.738	7.42
Midmyocardial apical CS	−0.060	−1.733	1.613	4.40
Epicardial apical CS	0.063	−1.113	1.239	4.25
Endocardial LS	0.030	−0.804	0.864	2.26
Midmyocardial LS	0.038	−0.670	0.746	2.13
Epicardial LS	0.081	−0.696	0.858	2.57
Torsion	−0.066	−1.733	1.613	4.40

CV, coefficient of variation; CS, circumferential strain; LLA, 95% lower limit of agreement; LS, longitudinal strain; ULA, 95% upper limit of agreement.

LV Torsion Pattern

Peak torsion was smaller in the T2 and T3 groups than in the C2 and C3 groups because of smaller peak apical rotation. Only one (1.5%) patient from the T2 group had an abnormal positive basal rotation (**Figure 2**, **Table S1**).

Torsion, Rotation, and LV Layer-Specific Strain: Relationship With RVEDA/BSA and RVFAC

Basal, papillary, and apical CS values, as well as LS in all 3 layers correlated with RVFAC (**Table 3**). Basal, papillary, and apical CS values, as well as LS in all 3 layers, excluding papillary epicardial CS, correlated with RVEDA/BSA (**Table 3**). Torsion and apical rotation in patients with TOF correlated with RVEDA/BSA and RVFAC, whereas there was no correlation with basal rotation (**Table 3**).

Reproducibility

Table 4 presents the results for intraobserver and interobserver variability. There were no important differences in the variability scores of the endocardial, midmyocardial, and epicardial CS at the basal, papillary, and apical levels or for LS.

Discussion

This is the first study showing the layer-specific strain parameters in patients with rTOF. The main findings of this study are as follows. (1) When focused on the same plane, impairment of LV peak strain occurs from the endocardial CS during the first decade after surgery, and subsequently expands towards the epicardial CS starting in the second decade after surgery in patients with rTOF. (2) When focused on each of the 3 short-axis planes, impairment of CS begins at the basal level during the first decade after surgery and expands towards the apex starting in the second decade after surgery, reaching the apex in the third decade after surgery. (3) Impairment of apical rotation occurs during the second decade after surgery, resulting in LV torsion impairment in patients with rTOF.

LV Dysfunction Assessed by Conventional Echocardiographic Parameters

In this study, only 2 (3%) patients showed decreased LVEF, and only 5 (7.6%) showed decreased RVFAC at the time of evaluation. In another study with a median length of follow-up reaching more than 20 years and mean patient age of 30 years, LVEF decreased in 23.6% of the patients.[22] The timing at which echocardiography was performed is a substantial reason for this difference in conventional echocardiographic results, as the mean time at which echocardiography was performed was 13.9 years post-repair in our study, which is relatively shorter than in previous reports. Other published studies showed that an older age at repair was a powerful predictor of poorer late survival.[5,23,24]

The mean age at the time of TOF repair in this analysis was 2.29 years, with an age range of 0.3 years to 7 years, which is relatively young compared with that reported elsewhere.[22]

Time Course of the Decrease in Layer-Specific Strain

Our study's findings suggest that myocardial deformation decreases with age in patients with rTOF, starting from the endocardial layer and expanding to the epicardial layer when focused on the same plane, and from the basal level towards the apex when focused on each of the 3 short-axis planes. LS of the LV measured by 2D echocardiography is one of the strongest predictors of clinical outcomes in patients with rTOF.[12] Our findings support those of previous studies that found LS to be an earlier marker of LV preclinical dysfunction than EF, as the LS in all 3 layers started to decrease in the second decade after surgery in the present patients with rTOF, whereas there were no significant differences in LVEF between controls and patients with rTOF in the same age group.

Impairment of Endocardial CS Before Epicardial CS Several studies have suggested vulnerability in the endocardial layers. Hamada et al reported that endocardial CS is a powerful predictor of cardiac events in patients with chronic ischemic cardiomyopathy, showing a significant difference between endocardial CS and endocardial LS in the accuracy of predicting cardiac events in this group of patients.[16] Yu et al showed that in anthracycline-treated survivors of childhood cancers, subendocardial circumferential deformation is sensitive to anthracycline.[17] In a rabbit model of DM,[25] and in patients with ischemia[15] or hypertension,[26] the vulnerability of the endocardial layers has been proposed. Although vulnerability of the endocardial layers in patients with rTOF has not been clarified physiologically or pathologically, the present study's findings demonstrated that potential myocardial damage occurs in the endocardial layers before the midmyocardial and epicardial layers in patients with rTOF when measured with layer-specific strain analysis, which is concordant with findings in reports on other diseases.

Impairment of Basal CS Before Apical CS As Streeter et al reported, the rate of circumferentially to longitudinally oriented fibers is 10:1, with its ratio increasing towards the base and decreasing towards the apex.[27] This suggests that the effect of impaired contraction in the circumferential direction is more prominent at the basal level than at the apex, as the base constitutes a considerable fraction of the LV wall. Furthermore, the Laplace law supports the idea that the larger cavity radius at the base than the apex of the LV is more affected by interventricular pressure[28] in the heart with subclinical myocardial damage. These findings support our results that impairment in basal and papillary CS occurs before that of the apical CS.

Impairment of CS Before LS Interestingly, the importance of CS has been reported in various studies of young patients with rTOF. Orwat et al reported that in patients with rTOF with an average age of 16 years, the strongest prognostic marker was LVCS.[29] Li et al reported that in patients with rTOF and an average age of 5.4 years, LVCS decreases significantly compared with controls, but only decreases significantly in the septal LS, not the lateral LS.[30] These reports indicate that in young patients with rTOF aged up to their teens, LVCS is an essential tool for evaluating myocardial damage, and is a prognostic marker.

The wall of the human heart has a well-defined distribution of fibers, with the angle varying from approximately 90° (in the circumferential direction) at the inner surface to approximately −90° at the outer surface.[27] The angle of fibers at 15% inside the LV endocardium is only 20°, which suggests that damage to the inner layer may affect both the longitudinally and circumferentially oriented fibers.[27] Furthermore, the ratio of circumferentially to longitudinally oriented fibers increases towards the base and decreases towards the apex.[27] When myocardial damage occurs only in the endocardial layers, LS remains stable until the damage approaches the epicardial layers,[16] as myocardial deformation of each layer is dependent on active function within the layer and passive motion from adjacent layers.[31,32] These findings suggest that contraction impairment affects CS more than LS, especially in young patients when myocardial damage is not as severe.

Mechanisms of Decreased LV Deformation in Patients With TOF

Proposed mechanisms of the LV dysfunction in patients with rTOF include preoperative myocardial hypoxemia, myocardial fibrosis, LV dyssynchrony, RV dysfunction caused by PR and RVOT obstruction, and LV-RV interaction.[14,29,30,33,34] Biventricular interaction in patients with rTOF has been further hypothesized as related to myocardial crosstalk through the sharing of myocardial fibers between the ventricles.[34] Orwat et al reported a correlation between LV and RV global systolic strain in patients with rTOF; they showed the LV-RV interaction using strain analysis measured by cardiac magnetic resonance (CMR) imaging.[29] Cheung et al also reported that the increase in RVESA correlated with the decrease in LVCS, demonstrating LV-RV interaction in patients with rTOF.[34] As the myocardial damage in RV progresses over time, it expands to include the LV and becomes severe through the LV-RV interaction.

In the third decade after surgical repair, myocardial deformation of the apex significantly decreased in the current study, primarily because of LV apical impairment affected by RV apical impairment. Sheehan et al[35] demonstrated that the geometric changes of the RV caused by persistent volume overload caused by pulmonary valve regurgitation in patients with rTOF was associated with significant enlargement only at the apical level. They concluded that this apical RV dilatation may lead to distortion of apical LV geometry and altered fiber orientation at the apex of the heart at an average of 20 years after surgery.

Rotation and Torsional Behavior

In this study, impairment in torsion starting in the second decade after surgery was mainly caused by impairment in apical rotation. The LV has a myocardial architecture that is a transmural continuum between 2 helical fiber arrangements, in which a subendocardial fiber wraps in a right-handed helix and a subepicardial fiber wraps in a left-handed helix from the base to the apex.[36] The subepicardial fibers cause a counterclockwise rotation torque, which dominates the subendocardial torque, as the former have greater radii,[37] resulting in apical rotation and torsion. As the left-handed helix fiber is placed in the midmyocardium and epicardium, decreases in midmyocardial CS at the basal and papillary muscle levels in the T2 and T3 groups resulted in a decrease of both apical rotation and torsion.

Clinical Implications

The present study provides the first evidence of preferential impairment of endocardial CS at the basal and papillary muscle levels in patients with rTOF. Most other strain and torsion parameters are considered to be useful indicators of cardiac dysfunction in comparison with LVEF. These findings have important clinical implications, as earlier detection of potential myocardial damage allows for early therapeutic intervention for subclinical LV dysfunction, such as β-blocker treatment to prevent severe LV dysfunction over the long term. Furthermore, this parameter could be used as an early marker of the efficacy of medical therapy.

Study Limitations

First, this study included a small number of patients, so future studies with a larger sample size are needed to provide a robust conclusion regarding whether endocardial CS does reflect potential myocardial damage in patients with rTOF.

Second, though CMR imaging is well accepted as the gold standard for evaluating RV function and volume,[4,38,39] we did not use it to assess patients in this study. It was difficult to have healthy controls undergo CMR examination, because of the high cost, the requirement for sedation in young children, and low availability.[38] However, as RVEDA and RVFAC measured by 2D echocardiography show linear correlation with RV volume and EF measured by CMR,[40] RVEDA and RVFAC are considered useful tools for assessing RV function in the clinical setting.[41]

Third, this was a cross-sectional study, so to analyze the true effect of aging on LV deformation, a longitudinal follow-up study is needed. Another important factor to consider is that the age of surgery for TOF in our T3 group was older than that in the T1 and T2 groups; this difference may affect LV function. In future studies, cardiac function in the same aged patients should be examined to evaluate changes with aging.

Conclusions

This could be the potential myocardial damage was found in the endocardium at the basal and papillary levels of the LV in young patients with rTOF. Myocardial deformation decreases with age in patients with rTOF, extending from the endocardium to the epicardium and from the base to the apex. This could be reflect potential myocardial damage and the possible time course of LV dysfunction in patients with rTOF.

Funding Sources

None.

References

1. Apitz C, Webb GD, Redington AN. Tetralogy of Fallot. *Lancet* 2009; **374:** 1462–1471.
2. Valente AM, Gauvreau K, Assent GE, Babu-Narayan SV, Schreier J, Gatzoulis MA, et al. Contemporary predictors of death and sustained ventricular tachycardia in patients with repaired tetralogy of Fallot enrolled in the INDICATOR cohort. *Heart* 2014; **100:** 247–253.
3. Nollert G, Fischlein T, Bouterwek S, Böhmer C, Klinner W, Reichart B. Long-term survival in patients with repair of tetralogy of Fallot: 36-year follow-up of 490 survivors of the first year after surgical repair. *J Am Coll Cardiol* 1997; **30:** 1374–1383.
4. Babu-Narayam SV, Kilner PJ, Li W, Moon JC, Goktekin O, Davlouros PA, et al. Ventricular fibrosis suggested by cardiovascular magnetic resonance in adults with repaired tetralogy of Fallot and its relationship to adverse markers of clinical outcome. *Circulation* 2006; **113:** 405–413.
5. Murphy JG, Gersh BJ, Mair DD, Fuster V, McGoon MD, Ilstrup DM, et al. Long-term outcome in patients undergoing surgical repair of tetralogy of Fallot. *N Engl J Med* 1993; **329:** 593–599.
6. Chiu SN, Wang JK, Chen HC, Lin MT, Wu ET, Chen CA, et al. Long-term survival and unnatural deaths of patients with repaired tetralogy of Fallot in an Asian cohort. *Circ Cardiovasc Qual Outcomes* 2012; **5:** 120–125.
7. Chung Y, Wong SJ, Liang X, Cheung EWY. Torsional mechanics of the left ventricle in patients after surgical repair of tetralogy of Fallot. *Circ J* 2011; **75:** 1735–1741.
8. Davlouros PA, Kilner PJ, Harming TS, Li W, Francis JM, Moon JC, et al. Right ventricular function in adults with repaired tetralogy of Fallot assessed with cardiovascular magnetic resonance imaging: Detrimental role of right ventricular outflow aneurysms or akinesia and adverse right-to-left ventricular interaction. *J Am Coll Cardiol* 2002; **40:** 2044–2052.
9. Miyazaki A, Yamamoto M, Sakaguchi H, Tsukano S, Kagisaki K, Suyama K, et al. Pulmonary valve replacement in adult patients with severely dilated right ventricle and refractory arrhythmias after repair of tetralogy of Fallot. *Circ J* 2009; **73:** 2153–2142.
10. Ghai A, Silversides C, Harris L, Webb GD, Siu SC, Therrien J. Left ventricular dysfunction is a risk factor for sudden cardiac death in adults late after repair of tetralogy of Fallot. *J Am Coll Cardiol* 2002; **40:** 1675–1680.
11. Knauth AL, Gaudreau K, Powell AJ, Landzberg MJ, Walsh EP, Lock JE, et al. Ventricular size and function assessed by cardiac MRI predict major adverse clinical outcomes late after tetralogy of Fallot repair. *Heart* 2008; **94:** 211–216.
12. Diller GP, Kempny A, Liodakis E, Gonzalez RA, Inuzuka R, Uebing A, et al. Left ventricular longitudinal function predicts life-threatening ventricular arrhythmia and death in adults with repaired tetralogy of Fallot. *Circulation* 2012; **125:** 2440–2446.
13. Geva T, Sandweiss BM, Gauvreau K, Lock JE, Powell AJ. Factors associated with impaired clinical status in long-term survivors of tetralogy of Fallot repair evaluated by magnetic resonance imaging. *J Am Coll Cardiol* 2004; **43:** 1068–1074.
14. Fernandes FP, Manlhiot C, Roche SL, Grosse-Wortmann L, Slorach C, McCrindle BW, et al. Impaired left ventricular myocardial mechanics and their relation to pulmonary regurgitation, right ventricular enlargement and exercise capacity in asymptomatic children after repair of tetralogy of Fallot. *J Am Soc Echocardiogr* 2012; **25:** 494–503.
15. Becker M, Ocklenburg C, Altiok E, Füting A, Balzer J, Krombach G, et al. Impact of infarct transmurality on layer-specific impairment of myocardial function: A myocardial deformation imaging study. *Eur Heart J* 2009; **30:** 1467–1476.
16. Hamada S, Schroeder J, Hoffmann R, Altiok E, Keszei A, Almalla M, et al. Prediction of outcomes in patients with chronic ischemic cardiomyopathy by layer-specific strain echocardiography: A proof of concept. *J Am Soc Echocardiogr* 2016; **29:** 412–421.
17. Yu W, Li S, Chan GCF, Ha S, Wong SJ, Cheung YF. Transmural strain and rotation gradient in survivors of childhood cancers. *Eur Heart J Card Img* 2013; **14:** 175–182.
18. Zoghbi WA, Enriquez-Sarano M, Foster E, Grayburn PA, Kraft CD, Levine RA, et al. Recommendations for evaluation of the severity of native valvular regurgitation with two-dimensional and Doppler echocardiography. *J Am Soc Echocardiogr* 2013; **16:** 777–802.
19. Lang RM, Badano LP, Mor-Avi V, Afilalo J, Armstrong A, Ernande L, et al. Recommendations for cardiac chamber quantification by echocardiography in adults: An update from the American Society of Echocardiography and the European Association of Cardiovascular Imaging. *J Am Soc Echocardiogr* 2015; **28:** 1–39.
20. Leitman M, Lysyansky P, Sidenko S, Shir V, Peleg E, Binenbaum M, et al. Two-dimensional strain: A novel software for real-time quantitative echocardiographic assessment of myocardial function. *J Am Soc Echocardiogr* 2004; **17:** 1021–1029.
21. Takahashi K, Naami GA, Thompson R, Inage A, Mackie AS, Smallhorn JF. Normal rotational, torsion and untwisting data in children, adolescents and young adults. *J Am Soc Echocardiogr* 2010; **23:** 286–293.
22. Ait Ali L, Trocchio G, Crepaz R, Stuefer J, Stagnaro N, Siciliano V, et al. Left ventricular dysfunction in repaired tetralogy of Fallot: Incidence and impact on atrial arrhythmia at long term-

follow up. *Int J Cardiovasc Imag* 2016; **32:** 1441–1449.
23. Katz NM, Blackstone EH, Kirklin JW, Pacifico AD, Bargeron LM Jr. Late survival and symptoms after repair of tetralogy of Fallot. *Circulation* 1982; **65:** 403–410.
24. Hu DCK, Seward JB, Puga FJ, Fuster V, Tajik AJ. Total correction of tetralogy of Fallot at age 40 years and older: Long-term follow-up. *J Am Coll Cardiol* 1985; **5:** 40–44.
25. Qiao YY, Zeng M, Li RJ, Leng ZT, Yang J, Yang Y. Layer-specific myocardial strain analysis: Investigation of regional deformation in a rabbit model of diabetes mellitus during different stages. *Med Ultrason* 2016; **18:** 339–344.
26. Enomoto M, Ishizu T, Seo Y, Yamamoto M, Suzuki H, Shimano H, et al. Subendocardial systolic dysfunction in asymptomatic normotensive diabetic patients. *Circ J* 2015; **79:** 1749–1755.
27. Streeter DD, Spotnitz HM, Patel DP, Ross J Jr, Sonnenblick EH. Fiber orientation in the canine left ventricle during diastole and systole. *Circ Res* 1969; **24:** 339–347.
28. Attias D, Macron L, Dreyfus J, Monin JL, Brochet E, Lepage L, et al. Relationship between longitudinal strain and symptomatic status in aortic stenosis. *J Am Soc Echocardiogr* 2013; **26:** 868–874.
29. Orwat S, Diller GP, Kempny A, Radke R, Peters B, Kühne T, et al. Myocardial deformation parameters predict outcome in patients with repaired tetralogy of Fallot. *Heart* 2016; **102:** 209–215.
30. Li Y, Xie M, Wang X, Lu Q, Zhang L, Ren P. Impaired right and left ventricular function in asymptomatic children with repaired tetralogy of Fallot by two-dimensional speckle tracking echocardiography study. *Echocardiography* 2015; **32:** 135–143.
31. Shi J, Pan C, Kong D, Cheng L, Shu X. Left ventricular longitudinal and circumferential layer-specific myocardial strain and their determinants in healthy subjects. *Echocardiography* 2016; **33:** 510–518.
32. Sarvari SI, Haugaa KH, Zahid W, Bendz B, Aakhus S, Aaberge L, et al. Layer-specific quantification of myocardial deformation by strain echocardiography may reveal significant CAD in patients with non-ST-segment elevation acute coronary syndrome. *J Am Coll Cardiol Imaging* 2013; **6:** 535–544.
33. Moon TJ, Choueiter N, Geva T, Valente AM, Gauvreau K, Harrild DM. Relation of biventricular strain and dyssynchrony in repaired tetralogy of Fallot measured by cardiac magnetic resonance to death and sustained ventricular tachycardia. *Am J Cardiol* 2015; **115:** 676–680.
34. Cheung EWY, Liang X, Lam WWM, Chueng Y. Impact of right ventricular dilation on left ventricular myocardial deformation in patients after surgical repair of tetralogy of Fallot. *Am J Cardiol* 2009; **104:** 1264–1270.
35. Sheehan FH, Ge S, Vick GW III, Urnes K, Kerwin WS, Bolson EL, et al. Three-dimensional shape analysis of right ventricular remodeling in repaired tetralogy of Fallot. *Am J Cardiol* 2008; **101:** 107–113.
36. Vendelin M, Bovendeerd PH, Engelbrecht J, Arts T. Optimizing ventricular fibers: Uniform strain or stress, but not ATP consumption leads to high efficiency. *Am J Physiol Heart Circ Physiol* 2002; **283:** 1072–1081.
37. Ingels NB. Myocardial fiber architecture and left ventricular function. *Technol Health Care* 1997; **5:** 45–52.
38. Bernard Y, Morel M, Genon VG, Jehl J, Meneveau N, Schiele F. Value of speckle tracking for the assessment of right ventricular function in patients operated on for tetralogy of Fallot: Comparison with magnetic resonance imaging. *Echocardiography* 2014; **31:** 474–482.
39. Wald RM, Haber I, Wald R, Valente AM, Powell AJ, Geva T. Effects of regional dysfunction and late gadolinium enhancement on global right ventricular function and exercise capacity in patients with repaired tetralogy of Fallot. *Circulation* 2009; **119:** 1370–1377.
40. Kjaergaard J, Petersen CL, Kjaer A, Schaadt BK, Oh JK, Hassager C. Evaluation of right ventricular volume and function by 2D and 3D echocardiography compared to MRI. *Eur J Echocardiogr* 2006; **7:** 430–438.
41. Selly JB, Iriart X, Roubertie F, Mauriat P, Marek J, Guilhon E, et al. Multivariable assessment of the right ventricle by echocardiography in patients with repaired tetralogy of Fallot undergoing pulmonary valve replacement: A comparative study with magnetic resonance imaging. *Arch Cardiovasc Dis* 2015; **108:** 5–15.

Supplementary Files

Supplementary File 1

Table S1. Correlation of layer-specific strain between patients (T1–T3) and controls (C1–C3)

Please find supplementary file(s);
http://dx.doi.org/10.1253/circj.CJ-16-1162